

Relation of the superstructure modulation and extra-oxygen local-structural distortion in $\text{Bi}_{2.1-y}\text{Pb}_y\text{Sr}_{1.9-x}\text{La}_x\text{CuO}_z$

Mao Zhiqiang, Xu Gaojie, Zhang Shuyuan, Tan Shun, Lu Bin, Tian Mingliang, Fan Chenggao, and Xu Cunyi
Structure Research Laboratory, University of Science and Technology of China, Hefei, Anhui 230026, People's Republic of China

Zhang Yuheng

*Chinese Center of Advanced Science and Technology (World Laboratory), P.O. Box 8730, Beijing, People's Republic of China
 and Structure Research Laboratory, University of Science and Technology of China, Hefei, Anhui 230026, People's Republic of China*

(Received 9 September 1996)

The modulated structure of $\text{Bi}_{2.1-y}\text{Pb}_y\text{Sr}_{1.9-x}\text{La}_x\text{CuO}_z$ ($y=0.2, 0.4$; $0.1 \leq x \leq 1.0$) was studied by means of electron diffraction. The experimental data show that the modulated structure changes from a mixed Bi/Pb-type to a pure Bi-type modulation with an increasing amount of La content in both the $y=0.2$ and 0.4 series and that the periodicity of the Bi-type modulation decreases correspondingly. When $x=1.0$, the modulation exhibits nearly the same characteristic in the samples with $y=0.2$ and 0.4 . In addition, the extra-oxygen behavior, together with the local-structural distortion characteristic, related to the change of the modulated structure was also examined with Raman scattering, x-ray photoelectron spectroscopy and high-resolution electron microscopy. The experiment results reveal that there are more extra-oxygen atoms intercalating in the Bi_2O_2 layers with a decrease in the modulation periodicity in the $y=0.2$ series. However, for the $y=0.4$ series, no more extra oxygen is incorporated into the Bi_2O_2 layers with a decrease in the modulation periodicity, but the degree of local-structural distortion strengthens markedly in the Bi_2O_2 layers. Based on these experiment results, we discuss the relationship of the superstructure modulation, extra oxygen, and the local-structural distortion. [S0163-1829(97)00814-X]

I. INTRODUCTION

It is known that the Bi-based superconductors with the composition of $\text{Bi}_2\text{Sr}_2\text{Ca}_{n-1}\text{Cu}_n\text{O}_{2n+4+\delta}$, $n=1, 2$, and 3 ($n=1, 2201$; $n=2, 2212$; $n=3, 2223$) possess the superstructure modulation. The superlattice has orthorhombic symmetry in the 2212 and 2223 phases, but monoclinic symmetry in the 2201 phase. Regarding the origin of the modulated structure several models have been proposed, mainly including (1) the extra-oxygen model,¹⁻² (2) the crystal misfit model,³⁻⁵ (3) the ordering of Sr vacancies,⁶ (4) the regular substitution of Bi by (Ca, Sr) or Cu,⁷ and (5) the changes in the orientation of Bi lone pairs.¹ Among these models, the extra-oxygen model has been most widely accepted. It indicates that the periodic intercalation of extra-oxygen atoms in the Bi_2O_2 layers is responsible for the modulation and the extra oxygen is brought about by the partial substitution of Bi^{5+} for Bi^{3+} . The model is basically successful in explaining the variations of modulation periodicity caused by the substitution with different valence cations.^{8,9} For example, the partial substitution of La^{3+} for Sr^{2+} in $\text{Bi}_2\text{Sr}_2\text{CuO}_{6+\delta}$ leads to more extra-oxygen atoms intercalating into the Bi_2O_2 layers, thus decreasing the modulation periodicity, whereas the Pb^{2+} substitution for Bi^{3+} removes the extra oxygen from the Bi_2O_2 layers, therefore increasing the modulation periodicity.^{5,9}

However, the extra-oxygen model failed to explain the change of modulation caused by the substitution in Sr sites with the same valence cations [for instance, the Ba^{2+} substitution for Sr^{2+} (Ref. 5)], as well as the substitutions of $3d$ metals (Fe, Co, Ni, and Zn) for Cu.¹⁰ In addition, Pham *et al.*¹¹ reported that the samples with different oxygen con-

tent had modulated structures with the same modulation periodicity. They suggested that the presence of extra oxygen in the Bi_2O_2 layers could only be regarded as a consequence of the particular geometry induced by bismuth, but not as the origin of the modulation. Clearly the relation between the modulation and extra oxygen in the Bi_2O_2 layers has not yet completely been clarified. To further examine this relation, we recently studied the modulation structure of $\text{Bi}_{2.1-y}\text{Pb}_y\text{Sr}_{1.9-x}\text{CuO}_z$ ($y=0.2, 0.4$; $0.1 \leq x \leq 1.0$) and the related varying behaviors of the extra oxygen in the Bi_2O_2 layers. Our experimental results reveal that the characteristic of the superstructure modulation does not depend on the amount of the extra oxygen. The modulation can also appear in the compound with no extra oxygen. In this paper, we report on these results and discuss the relation of the superstructure modulation, extra oxygen, and the local-structural distortion using the crystal misfit model.

II. EXPERIMENTAL METHODS

Samples were prepared through the conventional solid-state reaction method. Powders of Bi_2O_3 , PbO , SrCO_3 , La_2O_3 , and CuO were mixed with nominal compositions of $\text{Bi}_{2.1-y}\text{Pb}_y\text{Sr}_{1.9-x}\text{La}_x\text{CuO}_z$ ($y=0.2, 0.4$; $x=0.1, 0.2, 0.35, 0.5, 0.7$, and 1.0) (each sample is denoted by Pb/La content below) and then preheated in air at $820\text{--}830^\circ\text{C}$ for 40 h with an intermediate grinding. Then the powders were pressed into pellets, sintered in air at $870\text{--}910^\circ\text{C}$ for 60 h and finally quenched in air.

An x-ray-diffraction (XRD) analysis was carried out with a Rigaku-D/max- γA diffractometer using monochromatic high-intensity $\text{Cu-K}\alpha$ radiation. Electron diffraction (ED)

TABLE I. Structural parameters of the $\text{Bi}_{1.9}\text{Pb}_{0.2}\text{Sr}_{1.9-x}\text{La}_x\text{CuO}_z$ series.

La content x	a (Å)	b (Å)	c (Å)	q_b/b (Pb)	q_b/b (Bi)
0.1	5.359	5.370	24.563		
0.2	5.368	5.380	24.494		
0.35	5.382	5.393	24.470	5.66	4.39
0.5	5.388	5.398	24.326		
0.7	5.401	5.438	24.259		4.32
1.0	5.427	5.458	23.914		4.0

analysis was done with an H-800 transmission electron microscope. High-resolution electron microscopy (HREM) was performed with a JEOL-2010 electron microscope, equipped with a side entry stage with a $\pm 15^\circ$ double tilt. For electron microscopy studies, thin specimens were obtained by the ion-milling method. Raman spectra were measured on a Spex-1403 Raman spectrophotometer using a backscattering technique. The 5145-Å line from an argon-ion laser was used as an excitation light source. All measurements were made at room temperature, and each spectrum shown was taken with refocusing on at least two different spots to assure reproducibility. The x-ray photoelectron spectroscopy (XPS) measurements were performed on a ESCALAB MKII surface analysis system. The samples were scraped before being transferred into the analysis chamber in a vacuum of 1×10^{-9} mbar.

III. EXPERIMENTAL RESULTS

A. XRD and ED analyses of the $\text{Bi}_{2.1-y}\text{Pb}_y\text{Sr}_{1.9-x}\text{La}_x\text{CuO}_z$ ($y=0.2, 0.4; 0.1 \leq x \leq 1.0$) samples

The XRD analyses of $\text{Bi}_{2.1-y}\text{Pb}_y\text{Sr}_{1.9-x}\text{La}_x\text{CuO}_z$ ($y=0.2, 0.4; x=0.1, 0.2, 0.35, 0.5, 0.7, \text{ and } 1.0$) show that there is no sign of second phases for each doped sample and that all the diffraction peaks can be indexed on the basis of an orthorhombic unit cell. From XRD data, the lattice parameters for each doped sample were calculated using a least-squares refinement. Table I and Table II summarize the obtained results. From Tables I and II, it can be seen that the La substitution for Sr increases the lattice parameters a and b , and decreases the parameter c in both $y=0.2$ and 0.4 series.

TABLE II. Structural parameters of the $\text{Bi}_{1.7}\text{Pb}_{0.4}\text{Sr}_{1.9-x}\text{La}_x\text{CuO}_z$ series.

La content x	a (Å)	b (Å)	c (Å)	q_b/b (Pb)	q_b/b (Bi)
0.1	5.355	5.362	24.473		
0.2	5.358	5.368	24.444		
0.35	5.359	5.354	24.435	6.78	4.16
0.5	5.363	5.366	24.314		
0.7	5.423	5.400	24.165		4.12
1.0	5.440	5.447	24.129		4.0

Figures 1(a)–1(c) show the [100]-zone-axis ED patterns of the samples $\text{Bi}_{1.9}\text{Pb}_{0.2}\text{Sr}_{1.9-x}\text{La}_x\text{CuO}_z$ ($x=0.35, 0.7, \text{ and } 1.0$). In the diffraction pattern of the sample 0.2/0.35, two sets of satellite reflection, forming two rectangular lattices, are observed. This suggests that two types of orthorhombic modulation coexist in this compound. The weaker satellite diffraction corresponds to the orthorhombic Pb-type modulation, which has been reported in Pb-doped Bi-2201, 2212, 2223 phases,^{12–14} and the stronger satellite diffraction to the orthorhombic Bi-type modulation. The periodicities along the b direction (q_b) of the two types of modulation are $5.66b$ (Pb-type) and $4.39b$ (Bi-type), respectively. In the samples 0.2/0.7 and 0.2/1.0, the Pb-type modulation disappears and only the Bi-type modulation exists. The superlattice remains an orthorhombic symmetry in the sample 0.2/0.7 but changes to the monoclinic symmetry in the sample 0.2/1.0. The modulation periodicities in the two samples decrease to $4.32b$ and $4.0b$, respectively.

The [100]-zone-axis ED patterns of the samples $\text{Bi}_{1.7}\text{Pb}_{0.4}\text{Sr}_{1.9-x}\text{La}_x\text{CuO}_z$ ($x=0.35, 0.7, \text{ and } 1.0$) are given in Figs. 2(a)–2(c), which show a similar change in the modulated structure with La content in the $y=0.4$ series as in the $y=0.2$ series. The modulated structure also changes from a mixed Bi/Pb type to pure Bi type with increasing amount of La content. The modulation periodicity data of the $y=0.4$ series are listed in Table II, which shows that the La substitution for Sr also decreases the periodicity of Bi-type modulation. The remarkable differences between the two series is that the modulation periodicity reduces more rapidly in the $y=0.4$ series than in the $y=0.2$ series and that the orthorhombic-monoclinic transition in the symmetry of su-

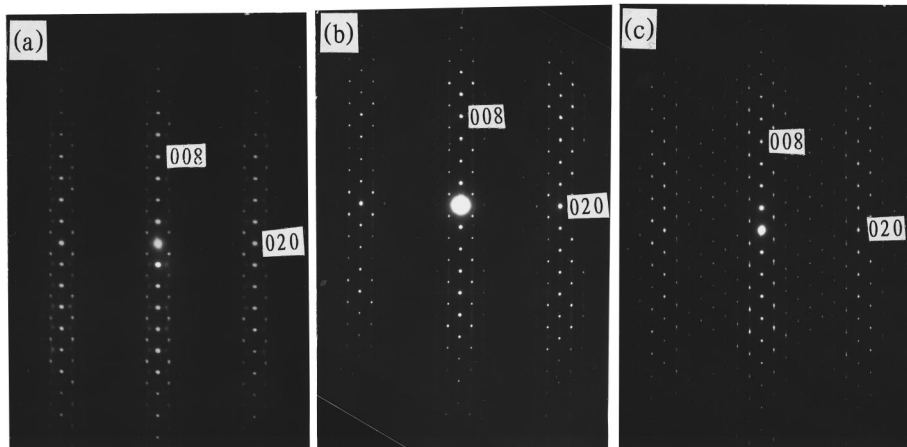


FIG. 1. ED patterns along the [100]-zone axis of the sample $\text{Bi}_{1.9}\text{Pb}_{0.2}\text{Sr}_{1.9-x}\text{La}_x\text{CuO}_z$; (a) $x=0.35$; (b) $x=0.7$; (c) $x=1.0$.

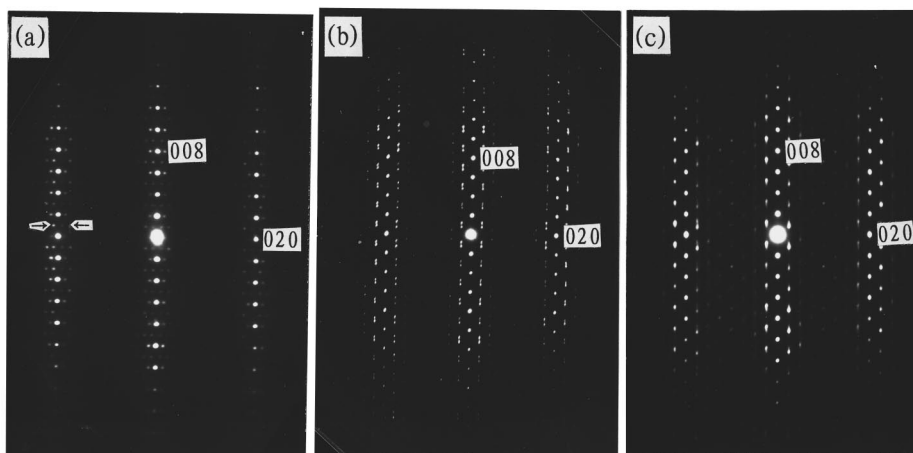


FIG. 2. (a) ED pattern along the $[100]$ -zone axis of the sample $\text{Bi}_{1.7}\text{Pb}_{0.4}\text{Sr}_{1.55}\text{La}_{0.35}\text{CuO}_z$, in which the double diffraction spots also appear (marked with arrows) besides the satellite diffraction reflecting the mixed Bi/Pb-type modulation. (b) ED pattern along the $[100]$ -zone axis of the sample $\text{Bi}_{1.7}\text{Pb}_{0.4}\text{Sr}_{1.2}\text{La}_{0.7}\text{CuO}_z$. All the satellite spots in this pattern are symmetric about the c^* or b^* axis. This type of b^*-c^* -plane ED pattern results from the two variants of structural modulation which are related by a symmetry plane (001), and a mirror plane is located at the bismuth oxide layer (Ref. 5). (c) ED pattern along the $[100]$ -zone axis of the sample $\text{Bi}_{1.7}\text{Pb}_{0.4}\text{Sr}_{0.9}\text{LaCuO}$.

per lattice occurs at much lower La content ($x < 0.7$) in the $y = 0.4$ series. On the other hand, it is worthwhile to note that the sample 0.4/1.0 almost shows the same characteristic in the modulated structure as the sample 0.2/1.0, i.e., monoclinic commensurate modulation with q_b of $4.0b$.

B. HREM analysis of the $\text{Bi}_{2.1-y}\text{Pb}_y\text{Sr}_{1.9-x}\text{La}_x\text{CuO}_z$ ($y = 0.2, 0.4; 0.1 \leq x \leq 1.0$) samples

Single-crystal XRD and HREM analyses have revealed that the modulation wave of the $\text{Bi}_2\text{Sr}_2\text{CuO}_{6+\delta}$ system causes swelling of each layer, i.e., the displacements of Bi, Sr, and Cu in the chains which run along the c axis.¹⁵⁻¹⁷ To examine this type of local structural distortion characteristic associated with the change in the modulated structure, we made HREM analyses for the $\text{Bi}_{2.1-y}\text{Pb}_y\text{Sr}_{1.9-x}\text{La}_x\text{CuO}_z$ system.

Figures 3(a)–3(c) show the HREM images projected along the a direction for the samples 0.4/0.35, 0.4/0.7, and 0.4/1.0. The double BiO layers (marked with a white arrow) and perovskite layers (marked with a black arrow) are well resolved in these images. From the micrograph of the sample 0.4/0.35 showing a mixed Bi/Pb-type modulation, it can be seen that the degree of bulking in the Bi, Sr, and Cu atomic chains is rather small, i.e., the local structural distortion is weak in this sample. Nevertheless, for the samples 0.4/0.7 and 0.4/1.0 showing a pure Bi-type modulation, the local structural distortion intensifies appreciably with a decrease in the modulation periodicity, as shown in Figs. 3(b) and 3(c). Especially in the sample 0.4/1.0, the arrangement of Bi atoms in the double BiO layers exhibits a very strong contracting and swelling behavior, thus forming obvious Bi-concentrated and Bi-deficient bands. In other words, a considerably strong local-structural distortion occurs in the Bi_2O_2 layers of this sample.

Figure 4 shows the $[100]$ HREM image of the sample 0.2/1.0. The ED analysis has indicated that this sample has nearly the same modulated structure as the sample 0.4/1.0. But, by comparing Fig. 4 with Fig. 3(c), we find that the degree of local structural distortion in the sample 0.4/1.0 is much stronger than that in the sample 0.2/1.0.

C. Raman scattering analysis of the $\text{Bi}_{2.1-y}\text{Pb}_y\text{Sr}_{1.9-x}\text{La}_x\text{CuO}_z$ ($y = 0.2, 0.4; 0.1 \leq x \leq 1.0$) samples

Figures 5(b) and 5(c) show the Raman spectra of the $\text{Bi}_{1.9}\text{Pb}_{0.2}\text{Sr}_{1.9-x}\text{La}_x\text{CuO}_z$ ($x = 0.1, 0.35, 0.5, 0.7, \text{ and } 1.0$) and

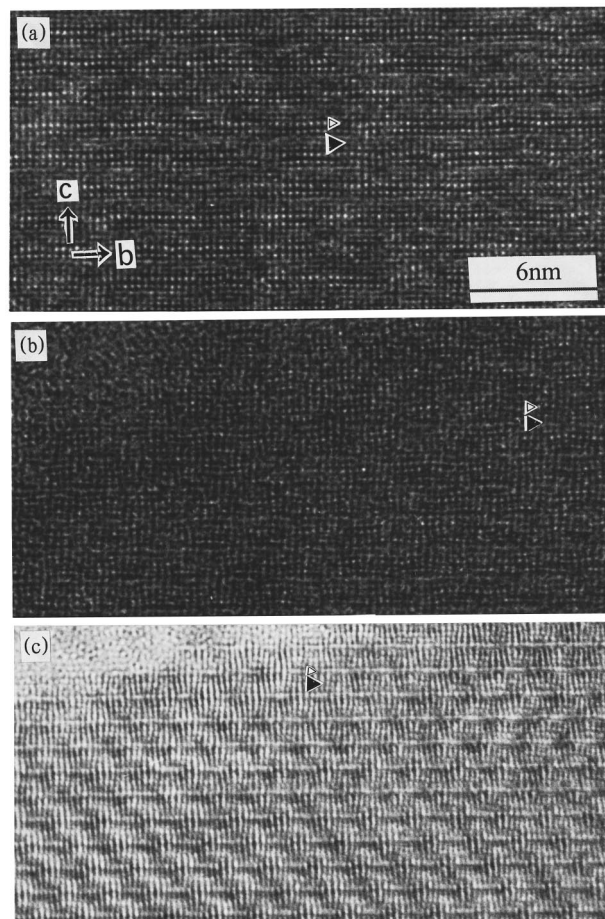


FIG. 3. $[100]$ HREM images of the sample $\text{Bi}_{1.7}\text{Pb}_{0.4}\text{Sr}_{1.9-x}\text{La}_x\text{CuO}_z$; (a) $x = 0.35$; (b) $x = 0.7$; (c) $x = 1.0$. The double BiO layer and perovskite block are marked with white and black arrows, respectively.

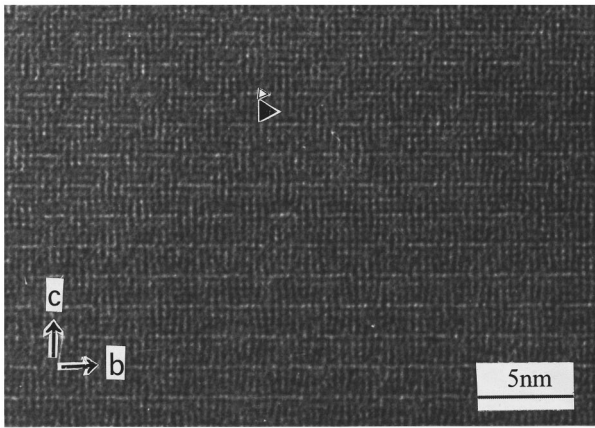


FIG. 4. [100] HREM image of the sample $\text{Bi}_{1.9}\text{Pb}_{0.2}\text{Sr}_{0.9}\text{LaCuO}_z$. The double BiO layer and perovskite block are marked with white and black arrows, respectively.

$\text{Bi}_{1.7}\text{Pb}_{0.4}\text{Sr}_{1.9-x}\text{La}_x\text{CuO}_z$ ($x=0.1, 0.35, 0.5, 0.7, \text{ and } 1.0$) samples in the frequency range $345\text{--}800\text{ cm}^{-1}$. Two Raman peaks are clearly observed within this frequency range for each doped sample. The peak with lower frequency ($450\text{--}470\text{ cm}^{-1}$) corresponds to the A_g mode of vibration of O_{Sr} atoms along the c axis, and the peak with higher frequency ($605\text{--}630\text{ cm}^{-1}$) to the A_g mode of vibration of O_{Bi} atoms along the a axis (O_{Sr} and O_{Bi} refer to the oxygen atoms in

the SrO and Bi_2O_2 layers, respectively).^{18,19} The O_{Sr} Raman peak shifts to the higher frequency side with increasing La content in both $y=0.2$ and 0.4 series, whereas the O_{Bi} Raman peak shifts to the lower frequency side. But the relative intensity of the O_{Sr} mode in the $y=0.4$ series is much lower than that in the $y=0.2$ series. On the other hand, the line shape of the O_{Bi} peak shows completely different variations with increasing La content between the two series. In the $y=0.2$ series, the O_{Bi} peak gradually splits into doublets, i.e., a shoulder peak appears around the higher frequency side of the main peak, and the relative intensity of the shoulder peak enhances apparently with increasing La content. Such a shoulder peak reflects the vibration of extra-oxygen atoms in the Bi_2O_2 layers.¹⁸ Hence, it can be considered that the La^{3+} substitution for Sr^{2+} brings more extra-oxygen atoms into the Bi_2O_2 layers in the $y=0.2$ series and the amount of extra oxygen grows with increasing La content. However, for the $y=0.4$ series, the most prominent change in the O_{Bi} peak is that its intensity reduces rapidly with increasing La content. The line shape of O_{Bi} peak is almost symmetric for each doped sample and no splitting behavior is observed even for the samples $0.4/0.7$ and $0.4/1.0$. This suggests that in the $y=0.4$ series the amount of extra oxygen is very small and that no more extra-oxygen atoms are incorporated into the Bi_2O_2 layers with the La^{3+} substitution for Sr^{2+} .

For the sake of comparison, we also give the Raman spectra of the Pb-free $\text{Bi}_{2.1}\text{Sr}_{1.9-x}\text{La}_x\text{CuO}_y$ system in Fig. 5(a)

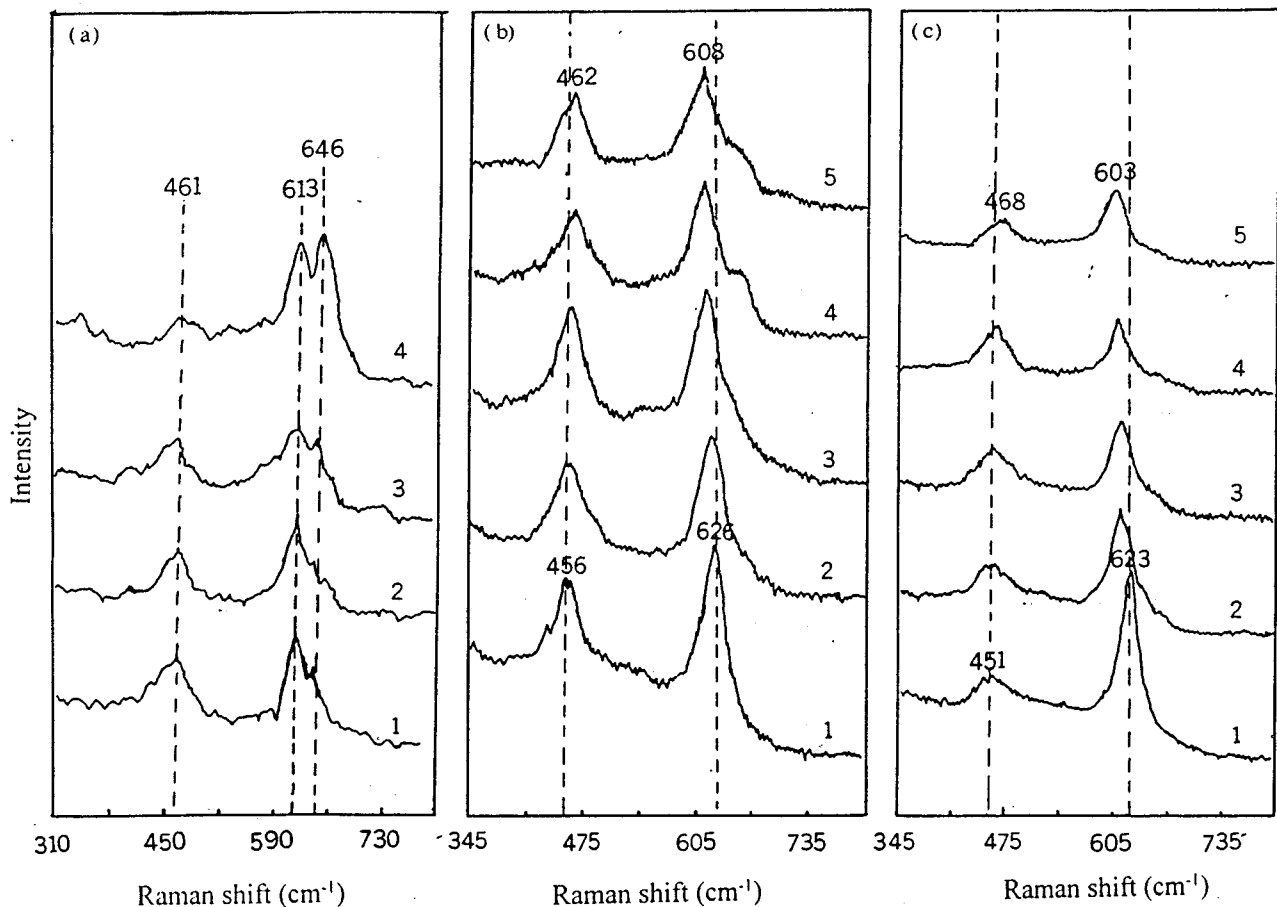


FIG. 5. (a) Raman spectra of the sample $\text{Bi}_{2.1}\text{Sr}_{1.9-x}\text{La}_x\text{CuO}_z$; 1, $x=0$; 2, $x=0.2$; 3, $x=0.6$; 4, $x=1.0$. (b) Raman spectra of the sample $\text{Bi}_{1.9}\text{Pb}_{0.2}\text{Sr}_{1.9-x}\text{La}_x\text{CuO}_z$; 1, $x=0.1$; 2, $x=0.35$; 3, $x=0.5$; 4, $x=0.7$; 5, $x=1.0$. (c) Raman spectra of the sample $\text{Bi}_{1.7}\text{Pb}_{0.4}\text{Sr}_{1.9-x}\text{La}_x\text{CuO}_z$; 1, $x=0.1$; 2, $x=0.35$; 3, $x=0.5$; 4, $x=0.7$; 5, $x=1.0$.

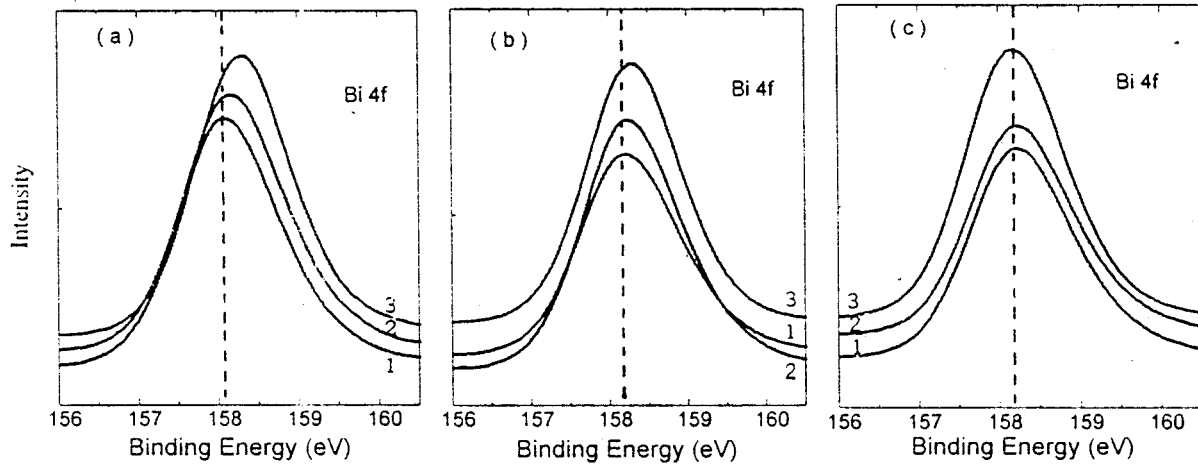


FIG. 6. (a) Bi 4*f* XPS spectra of the sample $\text{Bi}_{2.1}\text{Sr}_{1.9-x}\text{La}_x\text{CuO}_z$; 1, $x=0.1$; 2, $x=0.35$; 3, $x=1.0$. (b) Bi 4*f* XPS spectra of the sample $\text{Bi}_{1.9}\text{Pb}_{0.2}\text{Sr}_{1.9-x}\text{La}_x\text{CuO}_z$; 1, $x=0.1$; 2, $x=0.35$; 3, $x=1.0$. (c) Bi 4*f* XPS spectra of the sample $\text{Bi}_{1.7}\text{Pb}_{0.4}\text{Sr}_{1.9-x}\text{La}_x\text{CuO}_z$; 1, $x=0.1$; 2, $x=0.35$; 3, $x=1.0$.

(taken from our previous work⁹), which shows that both O_{Sr} and O_{Bi} phonon modes almost do not exhibit any shift in frequency and reduction in intensity with increasing La content. But the vibration mode of the extra-oxygen atoms in the Bi_2O_2 layers compared with the $y=0.2$ series intensifies much more strikingly with increasing La content. This suggests that for the samples with the same La content the amount of extra oxygen in the Bi_2O_2 layers of the $y=0.2$ series is notably smaller than that in the Pb-free series.

D. Analysis of XPS spectra for the $\text{Bi}_{2.1-y}\text{Pb}_y\text{Sr}_{1.9-x}\text{La}_x\text{CuO}_z$ ($y=0, 0.2, 0.4$; $0.1 \leq x \leq 1.0$) samples

Figures 6(a)–6(c) show the Bi 4*f* XPS spectra of the samples $\text{Bi}_{2.1-y}\text{Pb}_y\text{Sr}_{1.9-x}\text{La}_x\text{CuO}_z$ ($y=0, 0.2, 0.4$; $x=0.1, 0.35, \text{ and } 1.0$). The La^{3+} substitution for Sr^{2+} gives rise to an increase in the Bi 4*f* binding energy for both the $y=0$ and 0.2 series. But the increase in the Pb-free series is much more obvious than that in the $y=0.2$ series. Nevertheless, for the $y=0.4$ series, the Bi 4*f* binding energy almost remains intact when La content x increases from 0.1 to 1.0. These facts suggest that the Bi_2O_2 layers accept a large amount of extra oxygen introduced by the La^{3+} substitution for Sr^{2+} for the Pb-free system and a smaller amount for the $y=0.2$ series, while for the $y=0.4$ series no more extra oxygen is incorporated into the Bi_2O_2 layers with La^{3+} substitution for Sr^{2+} . This is in accord with the result obtained from the Raman-scattering analysis.

IV. DISCUSSION

From the above analyses, it can be seen that for the $\text{Bi}_{1.9}\text{Pb}_{0.2}\text{Sr}_{1.9-x}\text{La}_x\text{CuO}_z$ series the La^{3+} substitution for Sr^{2+} decreases the modulation periodicity and meanwhile brings a fraction of extra oxygen into the Bi_2O_2 layers. This implies that the decrease in the modulation periodicity is related to the increase of the extra oxygen in the Bi_2O_2 layers in this series, which can find a seeming interpretation from the extra-oxygen model. However, for the $\text{Bi}_{1.7}\text{Pb}_{0.4}\text{Sr}_{1.9-x}\text{La}_x\text{CuO}_z$ series, though each doped sample shows a strong modulated structure, the amount of the extra

oxygen in the Bi_2O_2 layers is much smaller compared with the $y=0$ and 0.2 series. Furthermore the decrease of the modulation periodicity is not accompanied with the increase of the extra oxygen. It is obvious that the extra-oxygen model cannot give a reasonable interpretation for the phenomena observed in the $y=0.4$ series, as well as the difference in the change of the modulated structure between the $y=0.2$ and 0.4 series.

On the other hand, we have already pointed out that the samples 0.2/1.0 and 0.4/1.0 have almost the same modulation structure. In fact, the $x=1.0$ sample in the Pb-free series (0/1.0) also possesses nearly the same modulation as the samples 0.2/1.0 and 0.4/1.0 (see Ref. 5). From the Raman spectra shown in Fig. 5 and the Bi 4*f* XPS spectra in Fig. 6, we can see clearly that the extra-oxygen behaviors among the three samples are completely different. A large amount of extra oxygen resides in the Bi_2O_2 layers in the sample 0/1.0, but only a small amount in the sample 0.2/1.0, and hardly any in the sample 0.4/1.0. These phenomena apparently indicate that the characteristic of the modulated structure does not depend on the amount of the extra oxygen in the Bi_2O_2 layers. For the $\text{Bi}_2\text{Sr}_2\text{CaCu}_2\text{O}_{8+\delta}$, as mentioned above, Pham *et al.*¹¹ have also obtained a similar result, i.e., the samples with different oxygen content exhibited the modulated structure with the same modulation periodicity. Evidently these behaviors are contradictory to the extra-oxygen model.

In our previous work, we found that the crystal misfit model is much more successful in explaining the modulation vector change induced by doping. As a matter of fact, the above-described phenomena which cannot be explained by the extra-oxygen model can be interpreted well in terms of the crystal misfit model. The earliest crystal misfit model was put forth by Gai, Subramanian, and Sleight.³ This model indicated that the superstructure modulation of Bi cuprates comes from the crystal misfit along the b axis between the Bi_2O_2 layer and perovskite block. The presence of extra-oxygen atoms in the Bi_2O_2 layers can be regarded as a consequence caused by the crystal misfit. We think that this type of intercalation of the extra oxygen in the Bi_2O_2 layers reduces the degree of the local structural distortion caused by the crystal misfit. The change in the modulated structure with

La content in both the Pb-free and Pb-doped ($y=0.2$ or 0.4) series can be considered to be a result of the enhancement in the degree of crystal misfit caused by the La^{3+} substitution for Sr^{2+} . For the Pb-free series, since a large amount of extra oxygen is incorporated into the Bi_2O_2 layers with a decrease in the modulation periodicity, the degree of the local structural distortion, especially in the Bi_2O_2 layers, should be rather small. The Raman spectra shown in Fig. 5(a) surely reflect this feature, i.e., the vibration modes of both O_{Sr} and O_{Bi} atoms do not exhibit a shift in frequency and reduction in intensity with a decrease in the modulation periodicity. Since the amount of extra oxygen introduced by the La^{3+} substitution for Sr^{2+} of the $y=0.2$ series is smaller than that of the Pb-free series, the amount of extra oxygen is not large enough to depress the local structural distortion and the degree of local structural distortion should intensify slightly with a decrease in the modulation periodicity. This postulation also agree well with the result shown in Fig. 5(b), in which a smaller frequency shift and intensity reduction caused by the enhancement in the local-structural distortion is detected in the vibration modes of the O_{Sr} and O_{Bi} atoms. Nevertheless, for the $y=0.4$ series, the decrease in the modulation periodicity is not accompanied with the intercalation of more extra oxygens, so it can be expected that the degree of local structural distortion should strengthen remarkably with a decrease in the modulation periodicity. The HREM images of the samples 0.4/0.35, 0.4/0.7, and 0.4/1.0 shown in Fig. 3 give a direct evidence of this expectation. Meanwhile the result of Raman spectra shown in Fig. 5(c) is also in accord with this expectation, namely a more striking frequency shift and intensity reduction for the O_{Sr} and O_{Bi} vibration modes with strengthening in the structural distortion are observed.

Based on the above analysis, it can naturally be postulated that the samples 0.2/1.0 and 0.4/1.0 should exhibit different features in the local-structural distortion though they have nearly the same modulated structure. The degree of local-structural distortion in the sample 0.4/1.0 with no extra oxy-

gen should be much larger than that in the sample 0.2/1.0 with a fraction of extra oxygen. The HREM images shown in Fig. 3(c) and Fig. 4 clearly reflect this kind of difference in the degree of local-structural distortion between these two samples.

V. CONCLUSION

We have studied the modulated structure of the $\text{Bi}_{2.1-y}\text{Pb}_y\text{Sr}_{1.9-x}\text{La}_x\text{CuO}_z$ ($y=0.2, 0.4; 0.1 \leq x \leq 1.0$) series, the extra-oxygen behavior and the local-structural distortion characteristic associated with the change in the modulation by means of XRD, ED, HREM, Raman scattering, and XPS. The relationship of the superstructure modulation, extra oxygen, and the local-structural distortion was discussed. From these experiments, investigations, and analyses, the following conclusions may be drawn.

(1) The characteristic of the modulated structure does not depend on the amount of the extra oxygen in the Bi_2O_2 layers, which implies that the modulation does not originate from the intercalation of the extra oxygen.

(2) The crystal misfit between the Bi_2O_2 layers and perovskite blocks should be the origin of the superstructure modulation. The intercalation of the extra oxygen weakens the local-structural distortion induced by the crystal misfit. The degree of local structure distortion is enhanced with a decrease in the amount of the extra oxygen in the Bi_2O_2 layers.

(3) The modulation can also appear in the Bi-based compounds with no extra oxygen. But the Bi_2O_2 layers are certain to exhibit a strong structure distortion in this case.

ACKNOWLEDGMENTS

This work was supported by the National Center for Research and Development on Superconductivity and the Foundation of National Education Ministry for Outstanding Young Teachers.

- ¹H. W. Zandbergen, W. A. Groen, F. C. Mijhoff, G. Tendeloo, and S. Amelinckx, *Physica C* **156**, 325 (1988).
- ²H. W. Zandbergen, W. A. Groen, A. Smit, and G. Tendeloo, *Physica C* **168**, 426 (1990).
- ³P. L. Gai, M. A. Subramanian, and A. W. Sleight (unpublished).
- ⁴X. B. Kan and S. C. Moss, *Acta Crystallogr. B* **48**, 122 (1992).
- ⁵Mao Zhiqiang, Fan Chenggao, Shilei, Yao Zhen, Yang Li, Wang Yu, and Zhang Yuheng, *Phys. Rev. B* **47**, 14 467 (1993).
- ⁶P. L. Gay and P. Day, *Physica C* **152**, 335 (1988).
- ⁷A. K. Cheetham, A. M. Chippendale, and S. J. Hibble, *Nature (London)* **333**, 21 (1988).
- ⁸H. Niu, N. Fukushima, S. Takeno, S. Nakamura, and K. Ando, *Jpn. J. Appl. Phys.* **28**, L784 (1989).
- ⁹Mao Zhiqiang, Zhang Hongguang, Tian Mingliang, Tan Shun, Xu Yang, Wang Yu, Zuo Jian, Xu Cunyi, and Zhang Yuheng, *Phys. Rev. B* **48**, 16 135 (1993).
- ¹⁰Mao Zhiqiang, Zuo Jian, Tian Mingliang, Xu Gaojie, Xu Cunyi, Wang Yu, Zhu Jingsheng, and Zhang Yuheng, *Phys. Rev. B* **53**, 12 410 (1996).
- ¹¹A. Q. Pham, M. Hervieu, A. Maigman, C. Michel, J. Provost, and B. Raveau, *Physica C* **194**, 243 (1992).
- ¹²Y. Matsui, A. Maeda, K. Uchinokura, and S. Takekawa, *Jpn. J. Appl. Phys.* **29**, 273 (1990).
- ¹³C. H. Chen, D. J. Werder, G. P. Espinosa, and A. S. Cooper, *Phys. Rev. B* **39**, 4686 (1989).
- ¹⁴S. Ikeda, K. Aota, T. Hatano, and K. Ogawa, *Jpn. J. Appl. Phys.* **27**, L2040 (1988).
- ¹⁵M. Onoda and M. Sato, *Solid State Commun.* **67**, 799 (1988).
- ¹⁶Y. Gao, P. Lee, J. Ye, P. Bush, V. Petricek, and P. Coppens, *Physica C* **160**, 431 (1989).
- ¹⁷O. Eibel, *Physica C* **168**, 215 (1990).
- ¹⁸M. Cardona, C. Thomsen, R. Liu, H. G. Vonscherner, M. Hartweg, Y. F. Yan, and Z. X. Zhao, *Solid State Commun.* **66**, 1225 (1988).
- ¹⁹R. Liu, M. V. Klein, P. D. Han, and D. A. Payne, *Phys. Rev. B* **45**, 7392 (1992).